

Characteristics of focused soft X-ray free-electron laser beam determined by ablation of organic molecular solids

J. Chalupský^{1,2,*}, L. Juha¹, J. Kuba², J. Cihelka^{1,3,4}, V. Hájková¹, S. Koptyaev¹, J. Krása¹, A. Velyhan¹, M. Bergh⁵, C. Coleman⁵, J. Hajdu⁵, R. M. Bionta⁶, H. Chapman⁶, S. P. Hau-Riege⁶, R. A. London⁶, M. Jurek⁷, J. Krzywinski⁷, R. Nietubyc⁸, J. B. Pelka⁷, R. Sobierajski⁷, J. Meyer-ter-Vehn⁹, A. Tronnier⁹, K. Sokolowski-Tinten¹⁰, N. Stojanovic¹⁰, K. Tiedtke¹¹, S. Toilekis¹¹, T. Tschentscher¹¹, H. Wabnitz¹¹, U. Zastra¹²

¹Institute of Physics, Academy of Sciences of the Czech Republic, Na Slovance 2, 182 21 Prague 8, Czech Republic

²Czech Technical University in Prague, Žitkova 4, 166 36 Praha 1, Czech Republic

³J. Heyrovský Institute of Physical Chemistry, Academy of Sciences of the Czech Republic, Dolejškova 3, 182 23 Prague 8, Czech Republic

⁴Charles University in Prague, Albertov 6, 128 43 Prague 2, Czech Republic

⁵Biomedical Centre, Uppsala University, Uppsala, SE-75124 Sweden

⁶Lawrence Livermore National Laboratory, 7000 East Avenue, Livermore, CA 94550, USA

⁷Institute of Physics, Polish Academy of Sciences, Al. Lotników 32/46, PL-02-668 Warsaw, Poland

⁸Soltan Institute for Nuclear Studies, PL-05-400 Swierk, Poland

⁹Max-Planck-Institut für Quantenoptik, Hans-Kopfermann-Str. 1, D-85748 Garching, Germany

¹⁰University of Duisburg-Essen, D-45117 Essen, Germany

¹¹Deutsches Elektronen-Synchrotron DESY, Notkestrasse 85, D-22603 Hamburg, Germany

¹²University of Jena, D-07743 Jena, Germany

*chal@fzu.cz

<http://www.fzu.cz>; <http://www.cvut.cz>

Abstract: A linear accelerator based source of coherent radiation, FLASH (Free-electron LASer in Hamburg) provides ultra-intense femtosecond radiation pulses at wavelengths from the extreme ultraviolet (XUV; $\lambda < 100\text{nm}$) to the soft X-ray (SXR; $\lambda < 30\text{nm}$) spectral regions. 25-fs pulses of 32-nm FLASH radiation were used to determine the ablation parameters of PMMA - poly (methyl methacrylate). Under these irradiation conditions the attenuation length and ablation threshold were found to be $(56.9 \pm 7.5)\text{ nm}$ and $\sim 2\text{ mJ}\cdot\text{cm}^{-2}$, respectively. For a second wavelength of 21.7 nm, the PMMA ablation was utilized to image the transverse intensity distribution within the focused beam at μm resolution by a method developed here.

©2007 Optical Society of America

OCIS codes: (140.7240) Lasers and laser optics: UV, XUV, and X-ray lasers; (140.2600) Lasers and laser optics: Free electron lasers; (340.0340) X-ray optics, (120.0120) Instrumentation, measurement, and metrology

References and links

1. P. E. Dyer, "Excimer laser polymer ablation: twenty years on," *Appl. Phys.* **A77**, 167-173 (2003) and references cited therein.
2. T. Lippert and J. T. Dickinson, "Chemical and spectroscopic aspects of polymer ablation: special features and novel directions," *Chem. Rev.* **103**, 453-485 (2003) and references cited therein.
3. Y. Zhang, "Synchrotron radiation direct photo-etching of polymers," *Adv. Polym. Sci.* **168**, 291-340 (2004) and references cited therein.
4. M. C. K. Tinone, K. Tanaka, and N. Ueno, "Photodecomposition of poly(methyl methacrylate) thin films by monochromatic soft x-ray radiation," *J. Vac. Sci. Technol.* **A13**, 1885-1892 (1995) and references cited therein.
5. L. Juha, J. Krása, A. Präg, A. Cejnarová, D. Chvostová, K. Rohlena, K. Jungwirth, J. Kravárik, P. Kubeš, Yu. L. Bakshaev, A. S. Chernenko, V. D. Korolev, V. I. Tumanov, M. I. Ivanov, A. Bernardinello,

- J. Ullschmied, and F. P. Boody, "Ablation of poly(methyl methacrylate) by a single pulse of soft X-rays emitted from Z-pinch and laser-produced plasmas," *Surf. Rev. Lett.* **9**, 347-352 (2002).
6. H. Fiedorowicz, A. Bartnik, M. Bittner, L. Juha, J. Krása, P. Kubát, J. Mikolajczyk, and R. Rakowski, "Micromachining of organic polymers by direct photo-etching using a laser plasma X-ray source," *Microelectron. Eng.* **73-74**, 336-339 (2004).
 7. L. Juha, M. Bittner, D. Chvostová, J. Krása, Z. Otcenasek, A. R. Präg, J. Ullschmied, Z. Pientka, J. Krzywinski, J. B. Pelka, A. Wawro, M. E. Grisham, G. Vaschenko, C. S. Menoni, and J. J. Rocca, "Ablation of organic polymers by 46.9-nm laser radiation," *Appl. Phys. Lett.* **86**, 034109 (2005).
 8. L. Juha, M. Bittner, D. Chvostová, J. Krása, M. Kozlová, M. Pfeifer, J. Polan, A. R. Präg, B. Rus, M. Stupka, J. Feldhaus, V. Létal, Z. Otcenasek, J. Krzywinski, R. Nietubyc, J. B. Pelka, A. Andrejczuk, R. Sobierajski, L. Ryc, F. P. Boody, H. Fiedorowicz, A. Bartnik, J. Mikolajczyk, R. Rakowski, P. Kubat, L. Pina, M. Horvath, M. E. Grisham, G. O. Vaschenko, C. S. Menoni, and J. J. Rocca, "Short-wavelength ablation of molecular solids: pulse duration and wavelength effects," *J. Microlith. Microfab. Microsyst.* **4**, 033007 (2005).
 9. T. Mocek, B. Rus, M. Kozlová, M. Stupka, A. R. Präg, J. Polan, M. Bittner, R. Sobierajski, and L. Juha, "Focusing a multimillijoule soft x-ray laser at 21 nm," *Appl. Phys. Lett.* **89**, 051501 (2006).
 10. V. Ayvazyan, *et al.*, "First operation of a free-electron laser generating GW power radiation at 32 nm wavelength," *Eur. J. Phys.* **D37**, 297-303 (2006).
 11. J. M. Liu, "Simple technique for measurements of pulsed Gaussian-beam spot sizes," *Opt. Lett.* **7**, 196-198 (1982).
 12. A. A. Sorokin, A. Gottwald, A. Hoehl, U. Kroth, H. Schöppe, G. Ulm, M. Richter, S. V. Bobashev, I. V. Domracheva, D. N. Smirnov, K. Tiedtke, S. Düsterer, J. Feldhaus, U. Jahn, U. Jastrow, M. Kuhlmann, T. Nunez, E. Plönjes, and R. Treusch, "Method based on atomic photoionization for spot-size measurement on focused soft x-ray free-electron laser beams," *Appl. Phys. Lett.* **89**, 221114 (2006).
 13. C. Valentin, D. Douillet, S. Kazamias, Th. Lefrou, G. Grillon, F. Aug, G. Mullot, Ph. Balcou, P. Mercere, and Ph. Zeitoun, "Imaging and quality assessment of high-harmonic focal spots," *Opt. Lett.* **28**, 1049 (2003).
 14. S. Kazamias, K. Cassou, O. Guilbaud, A. Klisnick, D. Ros, F. Plé, G. Jamelot, B. Rus, M. Kozlová, M. Stupka, T. Mocek, D. Douillet, P. Zeitoun, D. Joyeux, and D. Phalippou, "Homogeneous focusing with a transient soft X-ray laser for irradiation experiments," *Opt. Commun.* **263**, 98 (2006).
 15. P. Jaeglé, S. Sebban, A. Carillon, G. Jamelot, A. Klisnick, P. Zeitoun, B. Rus, M. Nantel, F. Albert, and D. Ros, "Ultraviolet luminescence of CsI and CsCl excited by soft x-ray laser," *J. Appl. Phys.* **81**, 2406 (1997).
 16. M. Kirm, A. Andrejczuk, J. Krzywinski, and R. Sobierajski, "Influence of excitation density on luminescence decay in $Y_3Al_5O_{12}:Ce$ and BaF_2 crystals excited by free electron laser radiation in VUV," *Phys. Stat. Sol.* **C2**, 649 (2005).
 17. S. Le Pape, Ph. Zeitoun, M. Idir, P. Dhez, J. J. Rocca, and M. François, "Electromagnetic-Field Distribution Measurements in the Soft X-Ray Range: Full Characterization of a Soft X-Ray Laser Beam," *Phys. Rev. Lett.* **88**, 183901 (2002)
 18. http://www.cxro.lbl.gov/optical_constants/getdb2.html

1. Introduction

PMMA ablation has been extensively investigated with conventional UV-Vis-IR lasers (see for example [1,2]). PMMA is also widely used in electron-beam, EUV, and x-ray lithography as a resist. Therefore its radiation-chemical and radiation-physical properties have been extensively studied and nowadays they are well understood over a wide range of irradiation conditions. PMMA erosion induced by high-energy photons (often also called direct photo-induced PMMA etching) in vacuum has already been investigated with synchrotron radiation [3,4] and with incoherent XUV/X-ray radiation from plasma-based sources [5,6]. Earlier studies [7-9] in the XUV laser-induced ablation of PMMA showed that the process is very clean. Furthermore, the PMMA material removal is governed by non-thermal processes and therefore restricted to the irradiation spot and its closest vicinity. These properties are the prerequisites for the characterization of focused soft x-ray laser beams using profile measurements of the crater created in PMMA.

In this article, we demonstrate the use of PMMA ablation to determine the focal spot intensity distribution of the new FLASH XUV free electron laser [10]. The article is organized as follows. In Section 2 we describe how the ablation threshold and the radiation attenuation length are determined for PMMA using Liu's method [11]. The extension of this method that enables us to determine the beam profile and the beam diameter at the focal spot is presented in Section 3. Finally, we summarize our experimental findings in Section 4.

2. Determination of ablation process and focal spot characteristics

Liu's method [11] utilizes surface damage to infer the focused beam characteristics. Linear behavior of the irradiated materials and strongly localized action of absorbed radiation energy are supposed. Initially we assume a Gaussian spatial shape of the FLASH pulses. The beam and material constants can then be calculated from fitting parameters A, B of a linear regression given by formulas $S = A + B \ln(E_{\text{pulse}})$ or $d = A + B \ln(E_{\text{pulse}})$ applied to measured crater areas S or crater depths d, respectively, as functions of the a pulse energy, E_{pulse} . For the area analysis the focal spot area S_{foc} and the ablation threshold F_{th} are related through [11]:

$$S_{\text{foc}} = B \quad (1a)$$

$$F_{\text{th}} = \exp(-A/B)/B \quad (1b)$$

Similarly, for crater-depth analysis the attenuation length l_{at} and ablation threshold F_{th} are given by [11]:

$$l_{\text{at}} = B \quad (2a)$$

$$F_{\text{th}} = \exp(-A/B)/S_{\text{foc}} \quad (2b)$$

We used 500-nm layers of 495K PMMA deposited on 315- μm -thick silicon chips fabricated by Silson, UK, in our experiments. The samples were positioned in an ultra-high vacuum interaction chamber and irradiated by single ≈ 25 -fs ≈ 10 - μJ FLASH pulses of 32-nm radiation. The beam was focused onto the sample by a grazing incidence elliptical mirror with a focal length of 2 m on Beamline 2. A ray tracing simulation suggested an expected focal spot diameter of 20 μm .

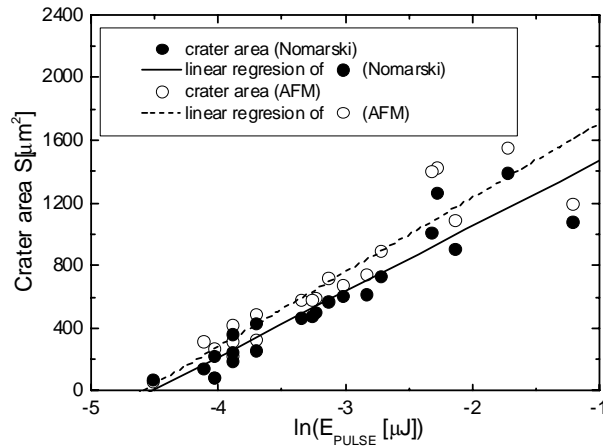


Fig. 1. Dependence of ablated PMMA area on FLASH pulse energy at 32 nm.

The ablated craters were investigated after the exposures by Nomarski (DIC – differential interference contrast) optical microscopy with BX51M DIC microscope (Olympus, Japan) and by atomic force microscopy (AFM) with a Dimension 3100 scanning probe microscope (SPM) driven by a NanoScope IV controller (Veeco, USA). The AFM measurement was carried out in a tapping mode.

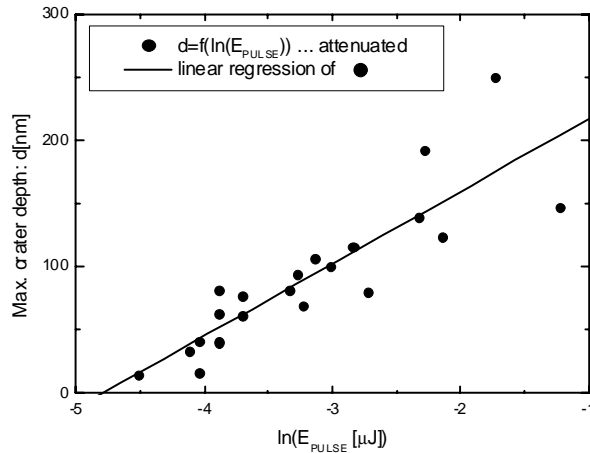


Fig. 2. Dependence of ablation depth in PMMA on FLASH pulse energy at 32 nm.

The results of our initial experiments carried out in Oct/Nov 2005 are presented in Figs. 1 and 2. Ablation and beam characteristics evaluated from these measurements according to Liu's method are summarized in the Table.

Table. Characteristics of FLASH-induced PMMA ablation at 32 nm.

ablation feature evaluated	type of microscope	ablation threshold F_{th} [mJ/cm ²]	attenuation length l_{at} [nm]	focal spot diameter 2ρ [μm]
crater area	DIC	(2.6±1.2)	---	(23.0±0.5)
	AFM	(2.1±1.1)	---	(24.6±0.6)
crater depth	AFM	(1.8±1.4)	(56.9±7.5)	---

The fluence required for single-shot PMMA ablation induced by 32-nm FEL radiation lies around 2 mJ·cm⁻². The attenuation length $l_{at} = (56.9 \pm 7.5)$ nm agrees well with the value of ~55 nm measured in PMMA with synchrotron radiation [16]. The tightly focused FLASH beam diameter, where the fluence drops to 1/e of its peak value, is $2\rho = (23.8 \pm 0.6)$ μm which is in a good agreement with the expected spot diameter calculated from the focusing system parameters and FLASH output characteristics, and experimentally determined using the atomic gas photo-ionization technique [12].

The PMMA ablation profile was smooth under the given irradiation conditions. There are no bubbles or any other surface imperfections attributed to PMMA thermal modification. The surface roughness as determined by means of AFM was (0.45±0.01) nm before irradiation, whereas the roughness increased to only (3.72±0.06) nm inside a typical crater, and was almost independent of fluence. Very low heat diffusivity $D \sim 0.001$ cm²/s of such a dielectric material together with ultra-short pulse duration $\tau = 25$ fs result in ultra-short heat diffusion length < 1nm [1]. Moreover, non-thermal processes play a key role in PMMA ablation induced by short-wavelength radiation. PMMA surfaces exposed to intense XUV/soft X-ray

radiation remain very smooth even if used source provides nanosecond and/or slightly sub-nanosecond pulses [6-9].

3. Beam profile reconstruction

The results shown above confirm that PMMA is a suitable material for investigation of the short-wavelength femtosecond laser beam ablative imprints. The ultra-low single-shot ablation threshold, smooth ablated surface, highly localized radiation action together with well satisfied Lambert-Beer's law make it possible to reliably and accurately reconstruct the transverse time-integrated intensity distribution in the XUV/soft X-ray laser beam from the AFM images for intensities down to the limiting PMMA threshold fluence, i.e., the major part of the beam carrying most of the pulse energy.

The Liu method assumes a Gaussian beam profile. We now extend this method to a more general beam profile. Let us suppose the incident field to be of a general form:

$$I(x, y, z, t) = I_0 \cdot f(x, y, z) g(t), \quad (3)$$

where z is a direction of light propagation, xy is a plane perpendicular to z parallel to the sample surface, $f(x,y,z)$ is a beam spatial intensity distribution, and $g(t)$ is a pulse temporal shape function. A sudden and well-localized response of a material to the ultra-short pulse radiation is assumed, thus slow thermal effects and low heat penetration are neglected. An experimental proof is shown in Fig. 3 where no feature characteristic for the thermal damage to the PMMA surface can be seen. This allows us to integrate over time thereby removing the time dependency. A spatial integral over the area xy gives the total pulse energy. Slowly varying envelope approximation (SVEA) in z -direction

$$\left| \frac{\partial f(x, y, z)}{\partial z} \right| \ll \left| l_{at}^{-1} f(x, y, z) \right| \quad (4)$$

allows us to neglect the intrinsic fluence variation along the z -axis between the sample surface ($z = 0$) and the crater bottom due to the large Rayleigh range of the beam (~ 1 mm) compared to the crater depth (~ 100 nm). Therefore, in z -direction, the fluence decreases down to the ablation threshold F_{th} following the Lambert-Beer law. The threshold fluence can be expressed as separate factors involving the crater shape $d(x,y)$ and beam profile $f(x,y,0)$:

$$F_{th} = F_0 f(x, y, 0) \exp(-d(x, y)/l_{at}). \quad (5a)$$

The transverse radiation energy distribution in the sample surface plane, $F(x,y,0)$, can then be expressed in terms of the measured attenuation length l_{at} , the ablation threshold F_{th} and crater profile $d(x,y)$ through Eq. (5b),

$$F(x, y, 0) = F_0 f(x, y, 0) = F_{th} \exp(d(x, y)/l_{at}) \quad (5b)$$

On the other hand, the crater profile may be predicted through the beam distribution function, which has been measured for certain XUV sources by various methods, e.g., scintillator-based imaging as reported in [13,14]. However, scintillator response is usually non-linearly dependent on the intensity of short-wavelength laser radiation [15, 16]. This may dramatically affect the XUV intensity distribution reconstructed from the luminescence signal. Therefore it is not easy to get reliable data on the transverse intensity distribution in the short-wavelength laser beam from such a method. Shack-Hartmann/CCD wave-front sensor [17] can also be used to determine such a distribution of XUV/x-ray lasers providing some additional information on the field.

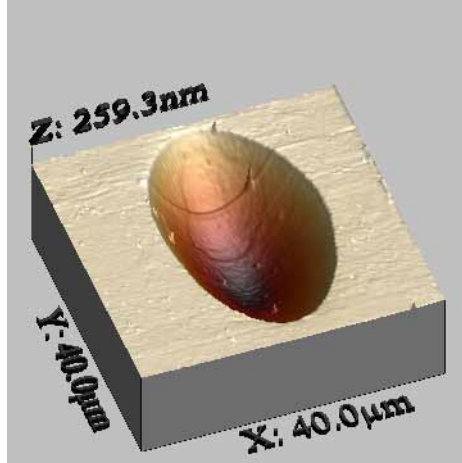


Fig. 3. A typical crater created in PMMA by the focused FLASH beam at 21.7 nm.

We found that the FLASH facility generates a roughly Gaussian beam creating craters with a paraboloidal shape that can be expressed in polar coordinates as:

$$d(r) = l_{at} \left(\ln \left(\frac{E_{pulse}}{E_{th}} \right) - \frac{r^2}{\rho^2} \right), \quad (6)$$

where $d(r)$ is the depth at radius r , ρ is a focal spot radius, E_{pulse} is the incoming pulse energy, and E_{th} is the threshold pulse energy.

Furthermore, it should be mentioned that the validity of these shape Eq. (5a), (5b), and (6) are restricted to the fluence range for which thermal and nonlinear effects are negligible. Radiation energy losses due to the surface reflectivity of PMMA were estimated to be less than 0.5% [18] and therefore ignored in our analysis.

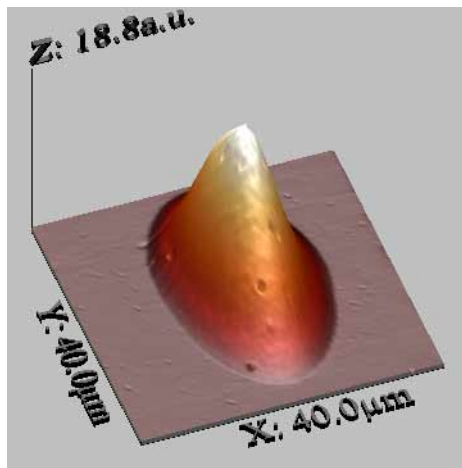


Fig. 4. The beam profile calculated from the AFM-measured shape of an ablated crater ablated by 21.7-nm radiation.

Reliable utilization of PMMA for post-exposure beam imaging has been proven in recent experiments in Sept 2006 conducted at the FLASH facility operated well into the soft x-ray spectral region, i.e., at wavelengths shorter than 30 nm. 1-mm thick samples of PMMA, manufactured by Goodfellow (UK), were irradiated with a tightly focused FLASH beam at

21.7 nm. The crater shapes observed by the AFM were elliptical paraboloids (Fig. 3). Equation (5) with an attenuation length of (69.9 ± 7.0) nm has been used to transform the 3-dimensional picture of a PMMA ablative crater to a 3D profile proportional to the real radiation field, focused by a 2-m elliptical grazing incidence mirror onto the sample surface, shown in Fig. 4.

Orthogonal cross-sections of the beam profile in the X and Y directions are shown in Fig. 5. Two different beam radii in the transverse directions can easily be recognized. The beam profile cross sections are well fitted by Gaussian functions with diameter values $2\rho_x = (11.8 \pm 1.0)$ μm and $2\rho_y = (21.4 \pm 1.6)$ μm . The diameter of the representative circular beam, calculated as a geometrical average of two values, is $2\rho = (15.8 \pm 1.4)$ μm and follows a decreasing trend with wavelength as compared to the 32 nm result. There are at least three reasons for this trend. The first one is coming from Gaussian beam feature $\rho \sim (\lambda)^{1/2}$, and the second one is related to the diffraction limit of the focusing optics $\rho \sim \lambda$. The third one is given by the increasing quality of the beam exiting the undulator as the electron energy (and thereby the photon energy) increases.

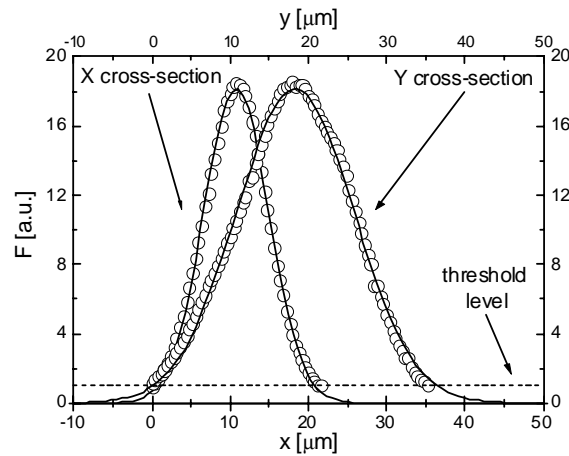


Fig. 5. Orthogonal beam profiles for 21.7 nm. The circles are the generalized solution based on Eq. (5b). The solid lines are Gaussian fits.

4. Conclusions

We have used a surface damage based method [11] to determine the focal spot size of tightly focused FLASH's beam lasing at 32 nm. The measured diameter of (23.8 ± 0.6) μm corresponds well to the results of photo-ionization measurements [12]. PMMA seems to be a suitable material for the beam characterization from an ablation crater because of strong localization of the photon action in the polymer structure. The low ablation threshold of PMMA irradiated by the FLASH beam (~ 2 mJ/cm² for 25-fs pulses at 32 nm) allows us to reconstruct a major part of the beam using the extended version of the method. Results obtained at 21.7-nm are also reported here. We observed an elliptical focal spot in which the intensity is well described by a bi-Gaussian function. A mean focal spot diameter of (15.8 ± 1.4) μm has been found at 21.7-nm, demonstrating increased beam focusing for the shorter wavelength.

Acknowledgments

This work was partially funded by the Czech Ministry of Education within the framework of programs INGO (Grant 1P2004LA235), 1K (Grant 1K05026) and National Research Centers (Grants LC510 and LC528), the Czech Academy of Sciences (Grant KAN300100702), State

Committee for Scientific Research of the Republic of Poland (Grant No72/E-67/SPB/5.PR UE/DZ 27/2003-2005), The Swedish Research Foundation and the European Commission (Grants G1MA-CI-2002-4017; CEPHEUS and RII3-CT-2004-506008; IA-SFS). This work was performed under the auspices of the US Department of Energy by the University of California, Lawrence Livermore National Laboratory under Contract No. W-7405-Eng-48.